PHYSICAL REVIEW A **78**, 061804(R) (2008)

Multiple-stream instabilities and soliton turbulence in photonic plasma

Dmitry V. Dylov and Jason W. Fleischer
Department of Electrical Engineering, Princeton University, Princeton, New Jersey 08544, USA
(Received 30 April 2008; published 24 December 2008)

We demonstrate weak and strong regimes of optical spatial turbulence by considering the nonlinear interaction of three partially coherent spatial beams. The geometry represents a multiple bump-on-tail instability, allowing an interpretation of nonlinear statistical light as a photonic plasma. For weak nonlinearity, we observe instability competition and sequential flattening of the bumps in momentum space, with no observable variations in position-space intensity. For strong nonlinearity, intensity modulations appear and the triple-hump spectrum merges into a single-peaked profile with an algebraic k^{-2} inertial range. This spectrum, with its associated modulations, is a definitive observation of soliton, or Langmuir, turbulence.

DOI: 10.1103/PhysRevA.78.061804 PACS number(s): 42.65.Sf, 42.68.Ay, 47.70.Nd, 52.35.Qz

The coupling of instabilities raises fundamental issues in nonlinear dynamics, such as synchronization, competition, parametric pumping, and cascades of energy and momentum transfer [1]. Examples range from predator-prey models in biology to laser synchronization to fluid turbulence. Here, we consider the common dynamics all-optically by studying the interaction of two photonic bump-on-tail instabilities [2], formed by the nonlinear coupling of three spatially incoherent light beams. By monitoring the spectral mode content in momentum space, we experimentally observe instability competition for weak nonlinearity and distribution merging for strong nonlinearity. These measurements highlight the difficulty of synchronized wave mixing inherent in noisy nonlinear systems and demonstrate a pathway toward all-optical studies of turbulence.

Previously thought to exist only in plasma, the bump-on-tail (BOT) instability is a gradient-driven effect in which a nonequilibrium bump on the tail of a thermal distribution acts as a source of free energy [3]. As such, it requires an inverted population of statistical modes and is often considered a type of classical lasing [4]. In plasma, the effect occurs when a gas of charged particles interacts through electrostatic, or Langmuir, waves. Recently, we showed that the same phenomenon could occur in the nonlinear propagation of statistical light, in which an ensemble of speckles interacts through large-scale modulation waves [2]. To see this, it is useful to consider a radiation-transfer approach to nonlinear light propagation. In the paraxial approximation, the statistical distribution of light evolves according to [5–8]

$$\frac{\partial f}{\partial z} + \beta \mathbf{k} \cdot \frac{\partial f}{\partial \mathbf{r}} + \frac{\partial \langle \Delta n(I) \rangle}{\partial \mathbf{r}} \cdot \frac{\partial f}{\partial \mathbf{k}} = 0, \tag{1}$$

where $f(\mathbf{r},\mathbf{k},z) = \frac{1}{2\pi}\int_{-\infty}^{+\infty} d\boldsymbol{\zeta} \langle \psi^*(\mathbf{r}+\boldsymbol{\zeta}/2,z) \cdot \psi(\mathbf{r}-\boldsymbol{\zeta}/2,z) \rangle e^{i\mathbf{k}\cdot\boldsymbol{\zeta}}$ is the phase-space (Wigner) distribution of the light, ψ is the slowly varying amplitude, $\beta = \lambda/2\pi n_0$ is the diffraction coefficient, n_0 is the base index of refraction, and Δn is the nonlinear index change induced by the local light intensity $I = I(x,y,z) = \int f(\mathbf{k}) d\mathbf{k}$. Normally, there is a second equation which describes the coupled evolution of Δn; here, we have jumped immediately to a time-averaged material response. The photorefractive crystal used for the experiments is such an inertial medium, in which $\langle \Delta n \rangle = \Delta n(\langle I \rangle_\tau)$ and fast phase fluctuations do not play a role.

Equation (1) contains the full nonlinear dynamics in $\{x,k\}$ phase space and resists general solution. Even qualitatively, the dynamics depends sensitively on the number of dimensions and the strength of the nonlinear coupling [9,10]. Here, we will concentrate on one dimension, consistent with the experiments described below, and begin by considering weak perturbations around an initial background distribution: $f(x,k_x,z) = f_0(k_x) + f_1 \exp[i(\alpha x - gz)]$, where $g = g_R + i g_I$ is the propagation constant for a perturbation mode with wave number α. Choosing a medium with an inertial Kerr response $\Delta n = \gamma \langle I \rangle_\tau$ (the case for the photorefractive nonlinearity, used in the experiments, is similar) gives the dispersion relation

$$1 = -\frac{\gamma}{\beta} \int_{-\infty}^{\infty} dk_x \frac{\partial f_0 / \partial k_x}{k_x - g/\alpha\beta}. \tag{2}$$

This is a Vlasov-like dispersion equation for the perturbation modes [7], showing that growth or decay depends on the local gradient of the background distribution. In particular, spectral regions with $\partial_k f_0 > 0$, such as a "nonequilibrium" bump on the tail of a Gaussian distribution, will trigger instability. In this Rapid Communication, we consider the evolution and competition of multiple instabilities by superimposing a set of Gaussian profiles. The simplest example is a central Gaussian distribution with M additional Gaussian beams, each with the same statistics (correlation length l_c), but positioned at different spatial frequencies (angular separations) δk_{01}, δk_{12}, δk_{23}, …, $\delta k_{M-1\ M}$:

$$f_0(k_x) = \frac{1}{\sqrt{2\pi}\Delta k} \left[I_0 e^{-k_x^2/2\Delta k^2} + \sum_{j=1}^{M} I_j e^{-(k_x - \delta k_{j-1j})^2/2\Delta k^2} \right]. \tag{3}$$

Here, $\Delta k = 2\pi/l_c$ is the full width at half maximum (FWHM) of each beam and $I_0, \ldots, I_M$ are individual amplitudes.

To study multiple bumps-on-tail instabilities, we plug (3) into (2) and use the weak growth condition $|g_I| \ll |g_R|$ to obtain

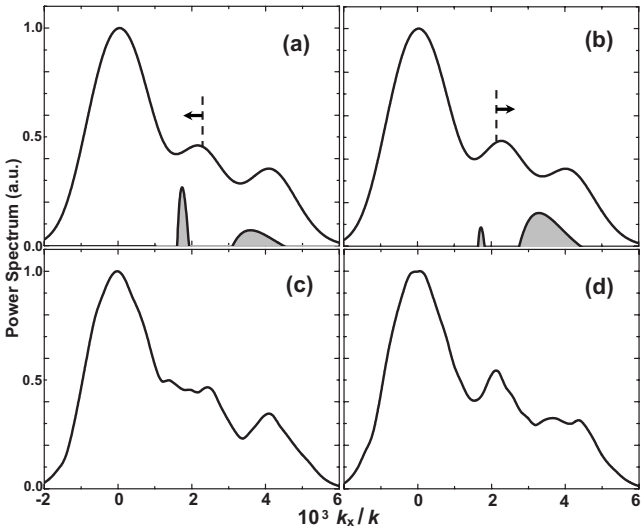

FIG. 1. Numerical simulation of multiple bump-on-tail instability. (a),(b) Input profiles, with corresponding gain curves (shaded graphs at the base line), with the middle hump shifted (a) to the left of the equal gain value and (b) to the right. (c),(d) Output pictures after 1 cm of propagation.

$$g = g_P\left(1 + \frac{3}{2}\alpha^2\lambda_D^2\right) + i\frac{\pi}{2}\gamma\alpha\sqrt{\frac{\gamma I_0}{\beta}}\left.\left(\frac{\partial f_0}{\partial k_x}\right)\right|_{k_x=g/\alpha\beta}. \quad (4)$$

where $g_P=\sqrt{\gamma\beta I_{tot}}$ is an effective plasma frequency that depends on the total nonlinear coupling $\gamma I_{tot}=\gamma\Sigma_{j=0}^{M} I_j$ and $\lambda_D = \sqrt{\frac{1}{\gamma\beta}\left(\frac{\Delta k^2}{I_{tot}}+\Sigma_{j=1}^{M}\frac{\delta k_{j-1j}^2}{I_j}\right)}$ is an effective Debye length that depends on the coupling and distribution of the beamlets. Equation (4), valid for long wavelengths $\alpha \ll g/(\beta k_x)$, is a Bohm-Gross dispersion relation [3] for nonlinear statistical light. It shows that a distribution f_0 of optical speckles can interact via Langmuir-type waves, with a restoration force that depends on the strength of the nonlinearity and a statistical screening that depends on the overall coherence of the distribution [2]. For an "equilibrium" background f_0, such as a quasithermal distribution of diffused light [11], perturbation modes will decay due to the optical equivalent of Landau damping [7,12–14]. For a "nonequilibrium" distribution—e.g., one with regions of positive spectral slope $(\partial f_0/\partial k_x > 0)$—modes will grow from noise with a rate that depends on the driving gradient, the statistics of the beam, and the strength of the wave coupling [2].

The dynamics within this photonic plasma depends on the spectral density of perturbation modes within a Debye sphere. For the weak-coupling regime considered above, defined by $\alpha\lambda_D < 1$ [12,13], the BOT instability is mostly a momentum-space effect [2]. Above this threshold, intensity modulations appear [12–14], wave-wave coupling (versus wave-speckle coupling) becomes dominant [2,10,15] and the perturbation method ceases to apply. Adopting plasma language, we define these two limits as regimes of weak and strong optical Langmuir turbulence.

As a first step, we consider two interacting bumps-on-tail in the weak-coupling regime. Figure 1 shows a numerical simulation of the dynamics and the corresponding gain

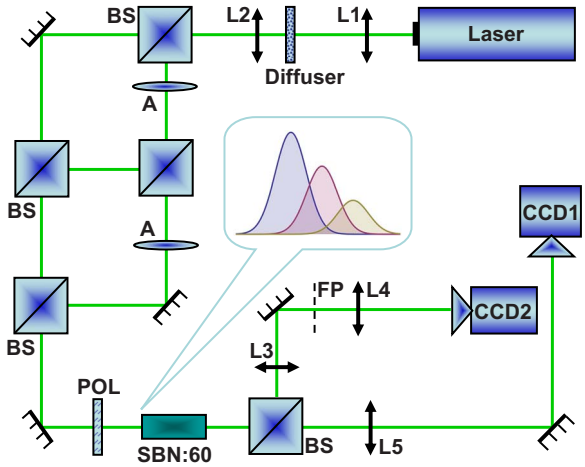

FIG. 2. (Color online) Experimental setup. Light from a 532-nm laser is made partially spatially incoherent by a ground-glass diffuser and separated into a superposition of three beams (inset). *A*, attenuator; *L*, lens; BS, beam splitter; POL, linear polarizer; SBN:60, nonlinear photorefractive crystal; FP, focal Fourier plane of the lens *L*3; CCD, digital detector.

curves calculated from Eq. (4). As expected, modes grow in the regions of positive spectral slope until there is no more driving gradient. We find that the system is described effectively as a pair of coupled BOT instabilities: one on the left and one on the right, with negligible coupling between the leftmost and rightmost Gaussians due to their separation distance. In this case, competition between the gain curves implies that plateau formation happens sequentially, even though the initial slopes and nonlinearity in the two regions are identical. If the middle hump is closer to the left (main) distribution, then the left region goes unstable first, and vice versa with a right bias [Figs. 1(c) and 1(d)]. The balanced situation, with the central hump equidistant from either side, has gain curves of the same peak value and is unstable. In simulations, this initial condition always degenerated into one of the two asymmetric scenarios, a result supported by analytic perturbations of δk_{01} in Eq. (4).

Experimentally, we observe this competition by considering the nonlinear interaction of three partially coherent spatial beams. The experimental setup is shown in Fig. 2. A statistical, quasithermal light input is created by focusing light from a 532-nm cw laser onto a ground-glass diffuser [11] and then imaging it into a photorefractive SBN:60 ($Sr_{0.6}Ba_{0.4}Nb_2O_6$) crystal. To create a multiple bump-on-tail distribution (Fig. 2, inset), the spatially incoherent beam is split using two Mach-Zehnder interferometers, attenuated appropriately, and then recombined on the input face of the crystal. These bumps, and the light polarization itself, are aligned along the crystalline *c* axis, so that the dynamics are effectively one dimensional (1D). Within the crystal, the nonlinear index change $\Delta n = \kappa E_{app}\langle I\rangle/(1+\langle I\rangle)$, where E_{app} is an electric field applied across the crystalline *c* axis and $\kappa = n_0 r_{33}(1+\langle I_0\rangle)$ is a constant depending on the base index of refraction n_0, the electro-optic coefficient r_{33}, and the spatially homogeneous incident light intensity $\langle I_0\rangle$ [16,17]. In the experiments, the beams have relative angles of $\sim 0.3°$ and $\sim 0.6°$, the sequential intensity ratios are fixed at ap-

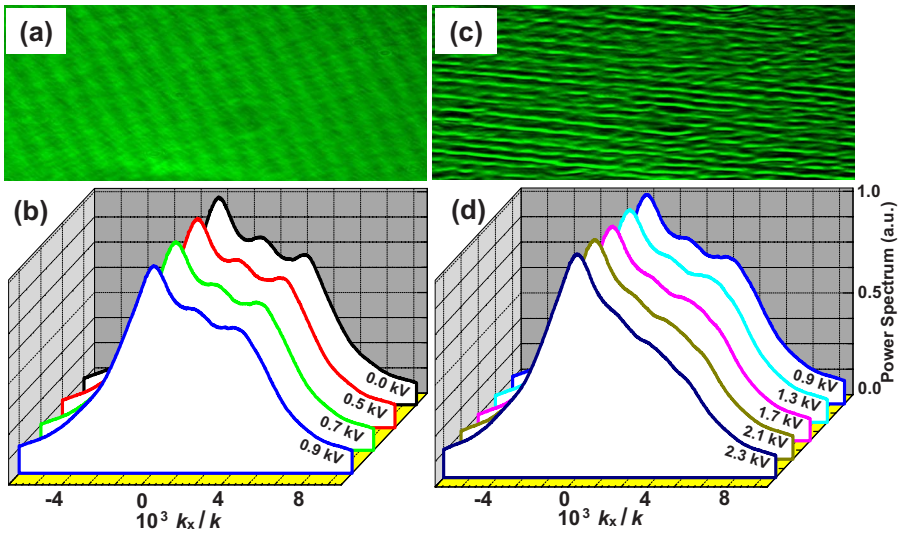

FIG. 3. (Color online) Experimental output pictures. Top row: intensity. Bottom row: power spectrum, as a function of nonlinear wave coupling (applied voltage across the crystal). (a),(b) Weak-coupling regime. (c),(d) Strong-coupling regime. Note that the slight modulations in intensity in (a) due to striations in the crystal do not affect the spontaneous modulations that appear in (c) above threshold.

proximately 3:2 to create equal slopes in the unstable regions, and the strength of the nonlinearity (wave coupling) is controlled by varying the applied voltage (similar results occur at other relative angles and intensities). To observe the interaction, light exiting the crystal is directly imaged in both position (**x**) space and momentum (**k**) space, the latter by performing an optical Fourier transform.

Experimental results for the weak-coupling case are shown in Figs. 3(a) and 3(b). The output intensity remained uniform, up to unavoidable striations in the crystal, while the energy spectrum underwent significant redistribution due to mode coupling. As the nonlinear interaction strength (applied voltage) was increased, the spectral bumps were observed to flatten. In all cases, the profile flattening was sequential, with lower momenta reaching a plateau first. This observation supports the general conclusion that the final state of the system depends on the temporal sequence of wave diffusion [18]. To our knowledge, this is the first demonstration of a multiple bump-on-tail instability and its associated competition of growth rates. Similar behavior should occur in any wave-kinetic system obeying Eq. (1), such as material plasma and cold atoms at finite temperature.

More complex behavior occurs for higher nonlinearity [Fig. 3(b)]. In the strong-coupling regime [2,12,13]—i.e., $\alpha\lambda_D \geqslant 1$—modulations start to appear in intensity and momentum transfer continues beyond the plateau (zero-gradient) limit [though the inertial approximation $\Delta n = \Delta n(\langle I \rangle_\tau)$ is still valid [2,14]]. In this case, the perturbed modes grow so quickly that wave-wave coupling is the dominant process of energy-momentum exchange [10,15]. A closer examination of this spectrum, shown in Fig. 4, reveals a self-similar profile with a k^{-2} falloff. This algebraic spectrum holds for the entire wave-number range between the first and last peaks, despite the fact that the central hump provided an initial region of stability ($\partial f_0 / \partial k < 0$).

The intensity waves present in the strong-coupling regime [Fig. 3(c)] are suggestive of solitons and, indeed, an ensemble of solitons can give the observed power spectrum [19]. For N solitons occupying a space of length L in 1D, having random phases and positions and maintaining total energy E_S, the Wigner spectrum $\langle f_k \rangle \propto \frac{1}{L}\int_{N_{\min}}^{N_{\max}} dN N \wp(N) [\cosh(kN/E_S)]^{-2}$, where $\wp(N)$ is the probability for the system to be in the N-soliton state and $N_{min} \leqslant N \leqslant N_{max}$ due to soliton merging and turbulent redistribu-

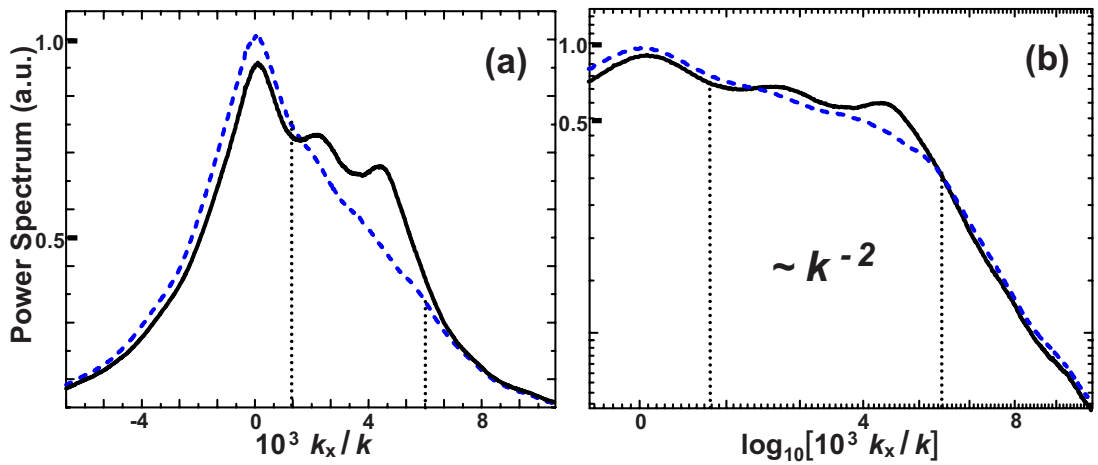

FIG. 4. (Color online) Asymptotic spectral profile of turbulent state. (a) Comparison of input (solid line) and output (dashed line) profiles. (b) Comparison in log-log space, showing the algebraic spectrum in the interaction region.

tion. Choosing $N_{max} \sim E_S/k$ (using the condition of close packing) and replacing the $\cosh^{-2}$ term by a step function yields $\langle f_k \rangle \propto \frac{1}{L} \int_{N_{\min}}^{E_S/k} dN N \wp(N)$. For the case when all states are occupied uniformly $[\wp(N) = \text{const}]$, $\langle f_k \rangle \propto k^{-2}$.

Interestingly, this particular equipartition spectrum is robust and appears in several different contexts of strong wave coupling. For example, dynamics with phase-dependent coupling—e.g., four-wave mixing—can give an effective wave collision term that leads asymptotically to a k^{-2} spectrum [20–22]. For the phase-independent coupling here, the intensity-induced interactions are enough to drive the dynamics. Indeed, similar conservation arguments on the photonic "plasmons" (speckles), rather than the number of solitons, also lead to a Rayleigh-Jeans distribution [20–22] $f_k = T/(k^2 - \mu)$, where the effective temperature $T \propto l_c^{-2}$ and the effective chemical potential is given by the average propagation constant (energy eigenvalue) of the waves. Note, however, that there must be a sufficient density of modes to achieve the equipartition. For few modes, relaxation can occur [23], but a self-similar spectral profile is not reached. Likewise, the presence of (incoherent) solitons—e.g., from modulation instability—is not enough to guarantee equipartition. There must be enough interaction and propagation distance (evolution time) to go beyond soliton clustering [24] and cascade the interactions [25,26]. Here, we encourage the wave-mixing cascade by seeding a "thermal" background distribution with additional "nonequilibrium" humps. The result is the first definitive proof, as measured by the power spectrum, of spatial optical turbulence.

In summary, we have demonstrated multiple bump-on-tail instabilities by considering the nonlinear propagation of spatially incoherent light as a photonic plasma. For weak nonlinearity, quasilinear flattening of the bumps in momentum space was observed to be sequential. For strong nonlinearity, merging of the spectral bumps into an algebraic k^{-2} power spectrum was observed. This profile, and the associated intensity modulations, is the hallmark signature of optical Langmuir turbulence.

This work was supported by the NSF, DOE, and AFOSR.

[1] T. Bohr, M. H. Jensen, G. Paladin, and A. Vulpiani, *Dynamical Systems Approach to Turbulence*, Cambridge Nonlinear Science Series Vol. 8 (Cambridge University Press, Cambridge, England, 1998).
[2] D. V. Dylov and J. W. Fleischer, Phys. Rev. Lett. **100**, 103903 (2008).
[3] N. A. Krall and A. W. Trivelpiece, *Principles of Plasma Physics* (McGraw-Hill, New York, 1973).
[4] V. Arunasalam, Am. J. Phys. **36**, 601 (1968).
[5] D. N. Christodoulides, T. H. Coskun, M. Mitchell, and M. Segev, Phys. Rev. Lett. **78**, 646 (1997).
[6] V. V. Shkunov and D. Z. Anderson, Phys. Rev. Lett. **81**, 2683 (1998).
[7] B. Hall, M. Lisak, D. Anderson, R. Fedele, and V. E. Semenov, Phys. Rev. E **65**, 035602 (2002).
[8] D. N. Christodoulides, E. D. Eugenieva, T. H. Coskun, M. Segev, and M. Mitchell, Phys. Rev. E **63**, 035601 (2001).
[9] S. L. Musher, A. M. Rubenchik, and V. E. Zakharov, Phys. Rep. **252**, 177 (1995).
[10] P. A. Robinson, Rev. Mod. Phys. **69**, 507 (1997).
[11] W. Martienssen and E. Spiller, Am. J. Phys. **32**, 919 (1964).
[12] A. A. Vedenov and L. I. Rudakov, Dokl. Akad. Nauk SSSR **159**, 767 (1964) [Sov. Phys. Dokl. **9**, 1073 (1965)].
[13] M. Soljacic, M. Segev, T. Coskun, D. N. Christodoulides, and A. Vishwanath, Phys. Rev. Lett. **84**, 467 (2000).
[14] D. Kip, M. Soljacic, M. Segev, E. Eugenieva, and D. N. Christodoulides, Science **290**, 495 (2000).
[15] M. V. Goldman, Rev. Mod. Phys. **56**, 709 (1984).
[16] M. Segev, G. C. Valley, B. Crosignani, P. Diporto, and A. Yariv, Phys. Rev. Lett. **73**, 3211 (1994).
[17] D. N. Christodoulides and M. I. Carvalho, J. Opt. Soc. Am. B **12**, 1628 (1995).
[18] N. J. Fisch and J. M. Rax, Phys. Fluids B **5**, 1754 (1993).
[19] A. S. Kingsep, L. I. Rudakov, and R. N. Sudan, Phys. Rev. Lett. **31**, 1482 (1973).
[20] S. Dyachenko, A. C. Newell, A. Pushkarev, and V. E. Zakharov, Physica D **57**, 96 (1992).
[21] V. M. Malkin, Phys. Rev. Lett. **76**, 4524 (1996).
[22] A. Picozzi, Opt. Express **15**, 9063 (2007).
[23] L. Levi, T. Schwartz, O. Manela, M. Segev, and H. Buljan, Opt. Express **16**, 7818 (2008).
[24] Z. G. Chen, S. M. Sears, H. Martin, D. N. Christodoulides, and M. Segev, Proc. Natl. Acad. Sci. U.S.A. **99**, 5223 (2002).
[25] V. N. Tsytovich (unpublished).
[26] S. I. Popel, V. N. Tsytovich, and S. V. Vladimirov, Phys. Plasmas **1**, 2176 (1994).